Available online at www.sciencedirect.com
ScienceDirect
C. R. Mecanique 336 (2008) 592–599
COMPTES RENDUS MECANIQUE
http://france.elsevier.com/direct/CRAS2B/

Relevance of a thermal contact resistance depending on the solid/liquid phase change transition for sprayed composite metal/ceramic powder by direct current plasma jets

Mohamed Bouneder, Mohammed El Ganaoui *, Bernard Pateyron, Pierre Fauchais

Université de Limoges, SPCTS – UMR 66 38 CNRS, Faculté des sciences et techniques, 123, avenue Albert-Thomas, 87060 Limoges, France

Received 2 September 2007; accepted after revision 22 April 2008

Available online 3 June 2008

Presented by Évariste Sanchez-Palencia

Abstract

The thermal contact between layers plays a key role in the behaviour of composite particles (mechanofused) subjected to a high temperature jet (example of two layers metal/ceramic particles under plasma spraying). This work underlines the interest of considering a thermal contact resistance varying with the melting state of the two components along the full process. The computational model considers the time-dependent state of the particle during its flight with coupled transfers and solid/liquid/vapor phase changes. ***To cite this article: M. Bouneder et al., C. R. Mecanique 336 (2008).***

Résumé

À-propos de la résistance thermique de contact et le changement de phase solide/liquide pour la projection des particules bicouche métal/céramique en projection plasma. Le contact thermique entre couches, joue un rôle important dans le comportement des particules composites à haute température (par exemple, les particules bicouches métal/céramique en projection plasma fabriquées par mécanofusion). Ce travail met en évidence l'intérêt de considérer un contact thermique fonction de l'état de fusion des deux couches sur l'ensemble du procédé de projection thermique. Le modèle prend en compte l'évolution de l'état de la particule le long de son parcours en couplant transferts et changements de phase solide/liquide/vapeur. ***Pour citer cet article : M. Bouneder et al., C. R. Mecanique 336 (2008).***

Keywords: Solid–liquid–vapor phase change; Two layer particles; Thermal contact resistance

Mots-clés : Changement de phase solide–liquide–vapeur ; Particules bicouche ; Résistance thermique de contact

* Corresponding author.
E-mail address: ganaoui@unilim.fr (M. El Ganaoui).

1631-0721/$ – see front matter
doi:10.1016/j.crme.2008.05.001

Version française abrégée

Le comportement thermique de particules, de taille de l'ordre de la dizaine de micromètres dans un jet gazeux à haute température, pose plusieurs défis sur les plans académique et industriel [1–3]. La projection thermique (Fig. 1) à haute température en est un exemple directement lié à l'industrie des procédés de traitement de surface. Ainsi une particule (typiquement 60 μm de diamètre) projetée dans un jet de gaz plasmagène Ar–H2 (typiquement à 10^4 K) est chauffée par conduction-convection et est soumise à des transitions de phase par fusion/solidification et par évaporation. En terme d'optimisation l'opérateur se trouve confronté à plusieurs paramètres de choix : puissance thermique de la torche, nature et débits des gaz plasmagènes, position du substrat, quantité de matière déposée, etc.

La déposition de particules composites bicouches, a fait l'objet d'études de faisabilité par simulation numérique pour la production de revêtements à Matrice Métallique Composite (MMC) ayant des propriétés mécaniques (résistance à la fatigue et à l'usure) intéressantes pour la fabrication de structures légères et renforcées (aéronautique, espace) ainsi que par la limitation de l'oxydation rencontrée en projection de poudre métallique à l'air libre [4–7]. En effet, l'exploitation d'un procédé en atmosphère contrôlée ou confinée implique un coût élevé pour l'industriel. L'appui de la modélisation et de la simulation numérique est ainsi le bienvenu dans ce domaine applicatif.

Généralement en présence de deux couches, en dépit du peu de réalisme physique attaché à cette hypothèse, les modèles d'interface utilisent une résistance thermique de contact constante [10]. En effet, en focalisant sur les autres phénomènes, un rôle mineur est attribué au contact. Le travail présenté montre l'insuffisance de cette modélisation. Le caractère rapide de l'évolution du phénomène étudié (de l'ordre de la milliseconde) et la présence de changement de phase suggèrent plutôt de tenir compte de la nature physique du contact thermique.

Ce travail est finalement dédié au traitement thermique de poudre composite bicouche métal/ céramique et avec une faible charge massique (débit d'injection moins de 1 kg/h) en projection par plasma d'arc soufflé Ar–H_2 75–25 % vol. L'influence de certains paramètres (taille, résistance thermique de contact, condition de chauffe) sur la cinétique du changement de phase et le procédé global est étudiée.

La Fig. 1 illustre l'interaction plasma/particule dans un procédé de projection thermique ainsi que l'observation par (Scanning Electron Microscopy) SEM [7] de particules fer/alumine collectées en vol. Les courbes de la Fig. 2 concernent la validation des modèles de fusion/solidification d'une sphère à travers d'une part la comparaison de l'évolution de la position du front de solidification dans le cas d'une condition de Dirichlet et du front de fusion dans le cas d'une condition de Robin. Suite à différentes étapes de validations, le développement aboutit à une prise en compte globale des transferts en présence de changement de phase dans chaque couche ainsi que la prise en compte du contact. La Fig. 3 reporte les phénomènes rencontrés le long d'une trajectoire. L'histoire thermique d'une particule de Fe/Al_2O_3 ($d_p = 60$ μm, $R_a/R_b = 0{,}93$, $R_{th} = 10^{-6}$ m^2K/W), est tracée pour une trajectoire optimale et les conditions de tir résumée au Tableau 1. La Fig. 4 reprend cette histoire thermique pour une résistance thermique de contact R_{th} (Éq. (5)) variable de 10^{-6} à 10^{-8} m^2 K/W. Ceci est complété par la Fig. 5 traçant les fractions liquides et le saut de température pour les deux cas de R_{th} constante et variable. Il en résulte une meilleure représentation du contact thermique dans le cas de R_{th} variable régularisant le profil d'évolution du saut thermique de part et d'autre de l'interface et réduisant sa durée dans le temps. Ceci est important pour la particule qui a particulièrement à supporter à la fois le saut de température et la durée de la persistance de ce saut vis-à-vis de son intégrité avant d'atteindre la cible.

1. Introduction

Understanding the thermal behaviour of a mechanofused composite metal/ceramic particle in a high temperature environment is essential for optimizing the plasma spray process. Thermal plasmas, used in spraying with temperatures in the order of 10^4 K provide very high heating rates to injected particles as well as high quench rates (10^6–10^8 K/s) for particles upon impact (Fig. 1). These aspects are of main significance for rapid solidification processes encountered in surface treatment.

Mono material particles have been extensively studied over the past decades [1–3]. Those constituted of two components have been subject of recent feasibility studies by using numerical simulation (see [4] and [5] in the case of infinite plasma). Such particles are used for producing Metallic Matrix Coating (MMC). The interest for mechanofused particles lies in the production of composite coating (metal matrix ceramic reinforced) less oxidized when sprayed in air [6].

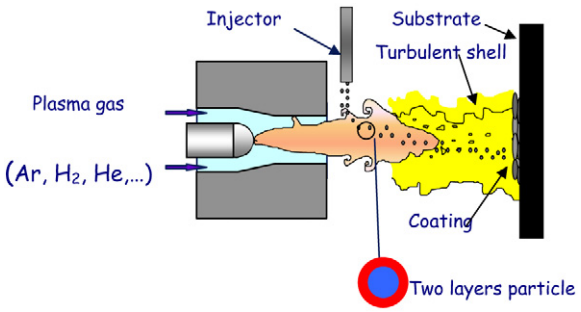

(a)

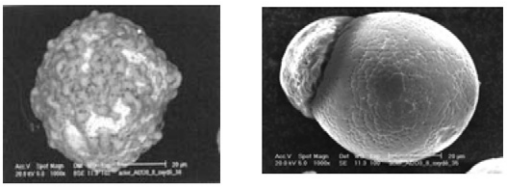

(b)

Fig. 1. Scheme of the spray process. (a) Sketch of the global setup. (b) Two layers particle collected in flight and observed by "Scanning Electron Microscopy SEM" [7].

Fig. 1. Schéma du procédé de projection thermique. (a) Schéma illustratif du dispositif. (b) Microscopie électronique à balayage (MEB) : configuration bicouche composite. MEB observation de particules Fer/alumine collectées en vol [7].

Quantitative knowledge of the thermal behaviour of a single composite metal/ceramic particles (as those obtained by the mechanofusion process [7]) and sprayed in a plasma jet is a key problem for optimizing the spray process. Metal particle with a ceramic shell have the potential for producing metal matrix composite coatings displaying better structural efficiency, protective wear at high temperature, enhanced material resistance against creep and crack failure and better resistance at high temperature environments.

Several coupled phenomena could be identified in this composite system referring to phase transition and solid/liquid/vapour interfaces. The relative behaviour of core/shell depends on the thermo-physical properties of the materials being considered, the composition of the plasma forming gas and their flow rate, the particle trajectory and the heat and mass transfer through the composite media is mainly driven by the physics of the contact between the metallic core and the ceramic shell.

This note presents computations following the particle along its trajectory within the plasma jet including coupled transfers with solid/liquid/vapour phase changes but focused on the interest of a contact model evaluating, through the melting state of the components, the global phenomena driving the particle history.

2. Thermal modelling

When considering heat and mass transfers in mono spherical particle, a few dimensionless numbers are sufficient to quantify and understand the phenomena, namely Biot, Fourier and Stefan (Bi, Fo and Ste respectively). For a plasma spray environment and a ceramic particle, the authors [10] show that the heat capacitance method (predominance of the capacitive effects) becomes valid for Biot number $\mathrm{Bi} < 0.03$ whereas in conventional problems, for example, a Biot number less than 0.1 typically implies that less than 5% error will be present when assuming a lumped-capacitance model of transient heat transfer [11]. So, full solution (space and time marching) is needed to treat the present problem, where alumina $\mathrm{Bi} > 0.03$.

For a mechanofused composite particle (metal core and ceramic shell), in addition to the preceding parameters, the interfacial thermal contact must be considered because it plays a key role in the heat exchanges. Other problems have also to be considered at high temperature (expansion coefficients mismatch, properties of both layers under phase change, ...). The consideration of the thermal contact quality can contribute to the quantification and the understanding of experimental observations such as the two types of particles collected in flight and presented in Fig. 1(b).

In the following, phase change has been modelled thanks to the Stefan problem for a double-layer composite sphere assuming that both material are homogeneous and isotropic with metal core (a) and ceramic shell (b), the solid–solid interface being noted Σ. The enthalpy model has been adopted for the formulation of the conservation equation of energy with phase change [5,8–10]. The melting or vaporization or solidification front position is thus a posteriori identified.

The numerical solution is based on the finite volume approximation developed to the second order accurate schemes in time and space. A thermal contact resistance (R_{th}) based on the solid volume fraction of the materials under consideration is proposed, to take into account solid–liquid transition. The thermal behaviour of the composite particle in the jet and along its trajectory is investigated and the influence of the main parameters such as the size of the particle, the ratio of the metal core to the ceramic shell, the thermo-mechanical properties and contact nature are clearly identified. Finally, some numerical results are obtained, which are in agreement with available experimental findings.

In spherical axisymmetric coordinates (r, ϑ, z) and with time t, one can write in each of the two layers:

$$\frac{\partial H}{\partial t} = \frac{1}{r^2}\frac{\partial}{\partial r}\left[k(T)r^2\frac{\partial T}{\partial r}\right] + \frac{1}{r^2\sin\theta}\frac{\partial}{\partial\theta}\left[k(T)\sin\theta\frac{\partial T}{\partial\theta}\right] \tag{1}$$

H is the specific enthalpy [J/kg], T the temperature [K], k the thermal conductivity [W/m K].

The initial and boundary conditions to be satisfied for the present model are:

At the centre, the mathematical problem associated with the temperature being multi-valued, problem removed by considering a very small but finite radius interior surface:

$$T(r, \theta, 0) = T_I$$

at

$$\vartheta = 0, \pi \tag{2}$$

$$\left[k_{\text{p}}(T)\frac{\partial T(r,\vartheta)}{\partial r}\right]_{r=R} = h_\infty(T_{\text{s}} - T_\infty) - \varepsilon\sigma T_{\text{s}}^4 - \dot{m}_{\text{v}}L_{\text{v}} \tag{3}$$

L is the specific heat [J/kg], h the exchange coefficient [W/m^2 K], ε is the emissivity and σ the Stefan–Boltzman constant ($= 5.671 \times 10^{-8}$ [W/m^2 K^4]). Subscript v refers to the vapour, eb to the ebullition, c to the centre ∞ to the plasma gas l to the liquid phase, s to the surface or solid phase, p to the particule, m to melting and 0 to the initial state.

The heat transfer coefficient is related to the Nusselt number by the Ranz and Marshall correlation modified for plasma media [2,12]:

$$h_\infty = \frac{\overline{k_\infty}}{d_{\text{p}}}\left[2 + 0.6Re^{0.5}Pr^{0.33}\right]\left((\rho\mu)/(\rho\mu)_{\text{sp}}\right)^{0.6}(C_{\text{p}}/C_{\text{p}_{\text{sp}}})^{0.38} \tag{4}$$

$\bar{k}$ is the mean integrated thermal conductivity [W/m K], ρ the specific mass [kg/m^3], d the diameter [m], c_{p} the specific heat [J/kg K]. Nu is the Nusselt number and Pr Prandtl number and Re Reynolds number. The heat flux conditions at the interface of two superposed materials is as follows:

$$\left[k_\alpha\frac{\partial T_\alpha}{\partial r}\right]_\Sigma = -\frac{\Delta T_\Sigma}{R_{\text{th}}}, \quad \alpha = a, b \tag{5}$$

In perfect contact case, the temperature jump at the interface is null (continuity of the thermal field).

The model considering R_{th} constant is physically insufficient because ignoring the nature of the contact between the layers in presence. To remedy to this insufficiency, a variable R_{th} model has been adopted accounting for the physical contact evolution during the solid/liquid transition.

Let f_{la} and f_{lb} refer to the liquid fractions respectively in the layer a and b. $f_{\text{lm}} = (f_{\text{la}} + f_{\text{lb}})/2$ is the average value. Considering a linear variation between R_{th1} for full solid ($f_{\text{sa}} = f_{\text{sb}} = f_{\text{sm}} = 1$) and a R_{th2} value traducing close to perfect contact (10^{-8} m^2 K/W) when the whole domain is liquid ($f_{\text{la}} = f_{\text{lb}} = f_{\text{lm}} = 1$) using the fact that liquids wet and allow better contact when filling interstitial pore and surface roughness.

$$R_{\text{th}}(f_{\text{lm}}) = (1 - f_{\text{lm}})R_{\text{th1}} + f_{\text{lm}}R_{\text{th2}} \tag{6}$$

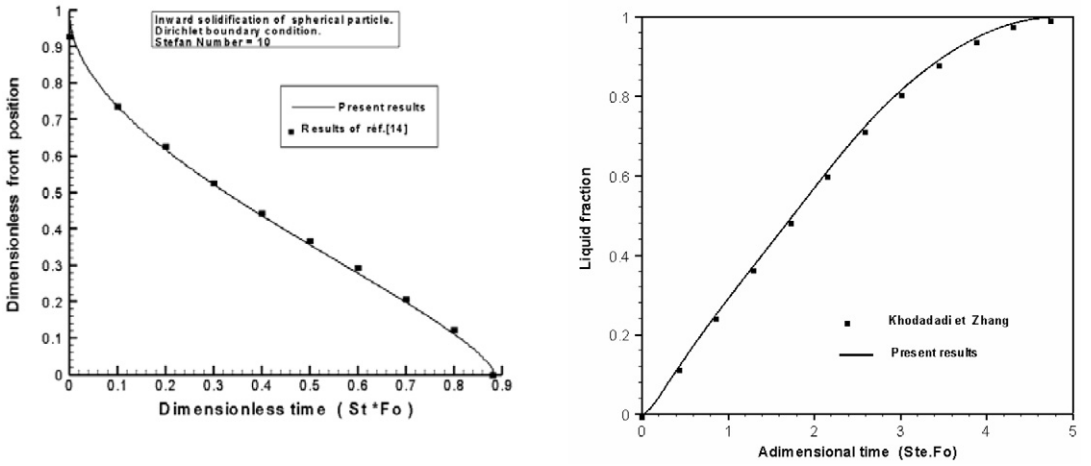

Fig. 2. Validation of the melting/freezing models within a sphere. Position of the melting front in the Dirichlet condition (left) and Robin condition (right).

Fig. 2. Validation des modèles de fusion/solidification d'une sphère. Comparaison de l'évolution de la position du front de solidification dans le cas d'une condition de Dirichlet (a) et de fusion dans le cas d'une condition de Robin (b).

According to the temperature range for particles (from 300 to 3000 K), physical properties are supposed to be temperature dependent [10].

3. Results and discussion

Full numerical solution is considered for the present problem to solve (1) accounting all conditions (2)–(6). First validations are reported then the model illustrates complex behaviours regarding composite particle thermal history along different trajectories in the plasma jet.

3.1. Validations

According to the difficulties to access to the experimental measurements related to a unique particle in such aggressive media with fast phenomena (particle residence time of a few ms), the model should describe the diffusive phenomena, as well as the various couplings with phase change. The numerical development has been validated with respect to a hierarchy of tests done (that are preferred to investigate phenomena separately). The cases of full melting or solidification in a homogeneous sphere are firstly investigated. Then phenomena along a thermal spray particle trajectory are considered. Strongly coupled phenomena are simulated after qualification of time and space grid dependency.

Accordingly, Fig. 2-left illustrates the validation of the solidification of a homogeneous sphere subjected to Dirichlet boundary conditions at its surface. Fig. 2-right shows the comparison to a sphere melting when submitted to Robin boundary conditions at its surface (Robin condition mixes Dirichlet and Neumann conditions). Other results for the vaporization model are reported in [10].

The model is then used for simulating coupled solid/liquid/vapour transitions during the spray process. The study of the time and space discretization permits to choose an optimal grid of $(N_r, N_\theta) = (100, 60)$ and a time step of $\Delta t = 1$ μs to be used for the following simulations.

3.2. Simulation along a trajectory and pertinence of the variable contact

Let recall to the reader that along its trajectory (from its injection in the plasma jet to the substrate), a single particle first is molten (completely or partially) and then can undergo vaporization (totally or partially). Into double-layered the relative behaviours of each layer with respect to the other one have to be considered (as well as the symmetry

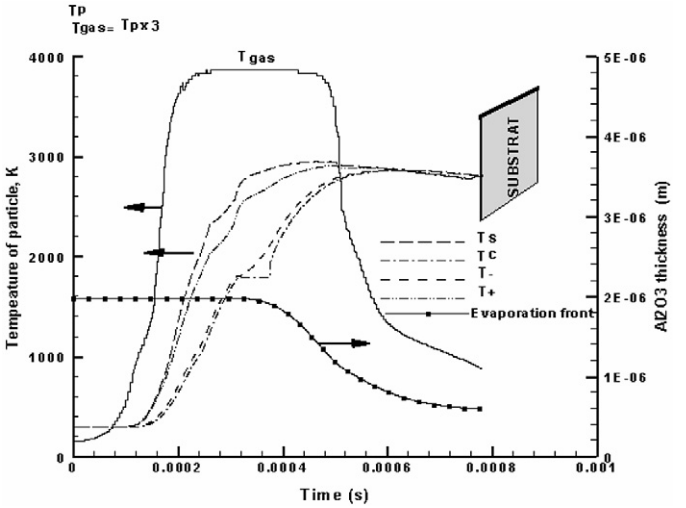

Fig. 3. Thermal history of a particle of Fe/Al_2O_3 ($d_p = 60$ μm, $R_a/R_b = 0.93$, $R_{th} = 10^{-6}$ m^2 K/W) for an optimal trajectory and the spray parameters of Table 1.

Fig. 3. Histoire thermique d'une particule Fe/Al_2O_3 ($d_p = 60$ μm, $R_a/R_b = 0{,}93$, R_{th} constante $= 10^{-6}$ m^2 K/W) trajectoire optimale et conditions de tir Tableau 1.

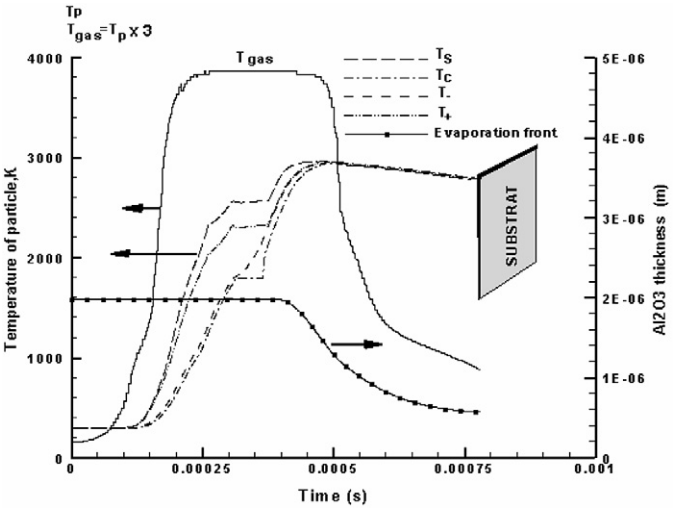

Fig. 4. Thermal history of a particle of Fe/Al_2O_3 ($d_p = 60$ μm, $R_a/R_b = 0.93$, R_{th} from 10^{-6} m^2 K/W to 10^{-8} m^2 K/W) for an optimal trajectory and spray parameters of Table 1.

Fig. 4. Histoire thermique d'une particule Fe/Al_2O_3 ($d_p = 60$ μm, $R_a/R_b = 0{,}93$, R_{th} variable de 10^{-6} à 10^{-8} m^2 K/W) trajectoire optimale et conditions de tir du Tableau 1).

breaking of the external layer and, its possible separation from the particle core). The contact has an important influence over characteristic times of the various phenomena, on the integrity of the particle upon impact and its state before flattening. By the way, thermal contact resistance is an important parameter for the transfers in double-layered particles. The jump of temperature estimated by calculation in the case of a double-layered particle with either of $R_{th} = 10^{-8}$ m^{2}K/W (perfect contact) ore with $R_{th} = 10^{-6}$ m^{2}K/W one (bad contact) can be about 300 K under spraying plasma conditions [10].

Figs. 3 and 4 show the evolution of plasma gas and temperatures of particles constituents (in each layer and through the contact line), as well as the vaporization front profile. Two thermal histories of the composite particle (shell alumina on a steel core Fe/Al2O3 60 μm in diameter and with $R_a/R_b = 0.93$) during its flight within the plasma

Table 1
Parameters of the plasma torch working conditions

Target distance [mm]	Current intensity [A]	Nozzle diameter [mm]	Argon flow rate [slm]	Hydrogen flow rate [slm]	Power [W]	Thermal efficiency [%]
10^{-2}	5×10^2	7	53	7	3×10^3	56

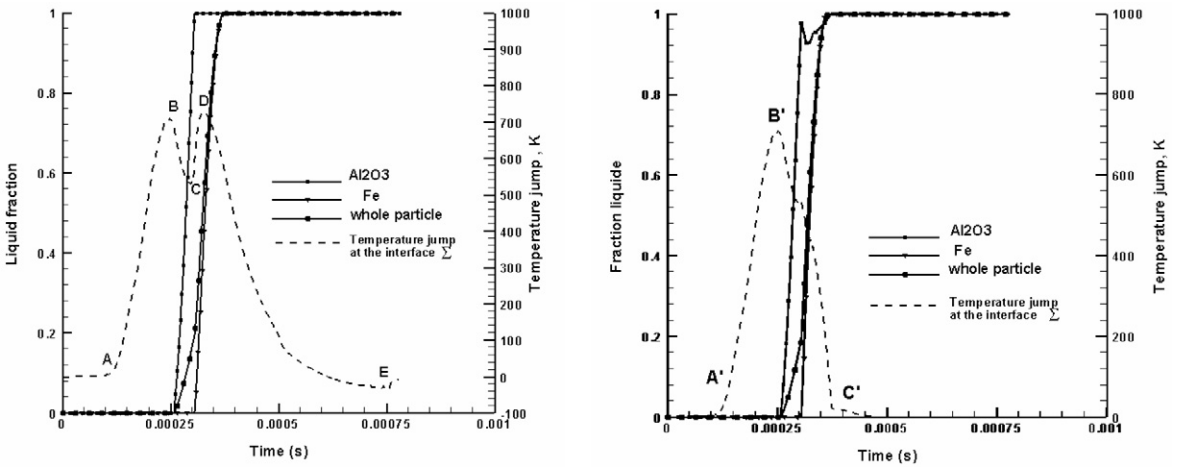

Fig. 5. Liquid fraction and temperature evolution (Fe/Al_2O_3, $d_p = 60$ µm, $R_a/R_b = 0.93$, $R_{th} = 10^{-6}$ m^2 K/W) and variation of R_{th} variable from 10^{-6} to 10^{-8} m^2 K/W, in optimal flight conditions and shot parameters from Table 1.

Fig. 5. Fractions liquides et saut de température (Fe/Al_2O_3, $d_p = 60$ µm, $R_a/R_b = 0{,}3$, R_{th} constante $= 10^{-6}$ m^2 K/W) R_{th} variable de 10^{-6}à 10^{-8} m^2 K/W, trajectoire optimale et conditions de tir Tableau 1.

jet are illustrating the purpose for both constant R_{th} (10^{-6} W m^2 K) and variable (10^{-6}–10^{-8} W m^2 K) (see parameters in Table 1).

The plasma gas temperature seen by the particle along its trajectory is represented by the near gaussian curve enveloping the others. Three zones are distinguished corresponding to: an initial rapid increase of temperature followed by a constant temperature plateau and after by a decrease of the temperature profile. The two last steps (plate and decreasing parts) are typically corresponding to the signature of classical jet flows [13]. The first step is more characteristic of the plasma and traduces the initial gas heating through the electric arc occurrence [1]. The global impact influences different characteristic times resulting on a global optimal time to reach the target. This estimate is a very useful operating parameter.

The particle temperature evolution, before phase change occurrence, is similar for the two assumptions on the thermal contact resistance. For the variable R_{th} model, phase change affects mainly the surface and the gaps both between the centre and the surface and through the interface. The composite sphere reaches a homogeneous temperature before leaving the plasma heating and is only evaporated at 20%. When this state reached for R_{th} constant model the particle is evaporated at 80% because its surface melting early allows evaporation in the first case. This history shows important differences in the heat transfers and phase change behaviours.

Fig. 5 shows the liquid fraction and temperature jump for both models. Two main observations can be made. The first one is the time during which the thermal gap is maintained through the interface (point A to point E in the curve (a)) two times longer than that obtained with the variable R_{th} case. The second observation is the behaviour of the gap which is more regular in the case of variable R_{th} (BCD in the curve (a)). This is important because the particle have to support this effort (the time duration of the gap and instability of heating) which directly may influence the mechanical properties and the integrity of the sprayed composite particle before reaching the substrate. Finally variable R_{th} has a regularizing effect on the gap and allows larger flying time.

4. Conclusion

This work highlights the interest of the modeling procedure on the control and the optimization of a complex process. It is particularly about the feasibility of tracking thermal histories of double-layer (core/shell) particles and underlines the interest of taking into account a contact between layers which is melting dependent. This stage is important before any extension to the thermo mechanical effects related to the expansion of the layers under the phase change occurrence and the modification of the contact between layers. Illustrations given here suggest the use of this model for other applicative problems involving transfers in heterogeneous media coupled to solid/liquid phase change.

References

[1] M.A. Vardelle, P. Fauchais, M.I. Boulos, Plasma-particle momentum and heat transfer: Modeling and measurements, AIChE (1983) 236–243.
[2] Y.C. Lee, E. Pfender, Particle dynamics and particle heat and mass transfer in thermal plasma 3. Thermal plasma – jet reactor and multiparticle injection, Plasma Chem. Plasma Process 7 (1987) 1–27.
[3] Y.P. Wan, V. Prasad, G.X. Wang, S. Sampath, J.R. Fincke, Model and powder particle heating, melting, resolidification, and evaporation in plasma spraying processes, J. Heat Transfer ASME 121 (1999) 691–699.
[4] M.D. Ghoniem, A.S. Lavine, N.M. Lavine, Feasibility of plasma spraying in developing MMC coatings: Modeling the heating of powder particles, J. Manuf. Sci. Eng. 124 (2002) 58–64.
[5] M. Bouneder, M. El Ganaoui, B. Pateyron, P. Fauchais, Coupled heat transfer modelling in composite (metal/ceramic) particle immersed in a plasma pool. Part II: Phase change, High Temp. Mat. Processes 9 (2005) 607–617.
[6] S.P. Rawal, Metal matrix composite for space applications, JOM 53 (2001) 14–17.
[7] H. Ageorges, P. Fauchais, Oxydation of stainless steel with and without an alumina shell during their flight in plasma, High Temp. Mat. Process. 4 (2000) 212–222.
[8] C.R. Swaminathan, V.R. Voller, On the enthalpy method, Int. J. Num. Meth. Heat Fluid Flow 3 (1999) 233–244.
[9] J.M. Khodadadi, Y. Zhang, Effects of buoyancy-driven convection on melting within spherical containers, Int. J. Heat Mass Transfer 44 (2001) 1605–1618.
[10] M. El Ganaoui, A. Lamazouade, P. Bontoux, D. Morvan, Computational solution for fluid flow under solid/liquid phase change conditions, Computers and Fluids 31 (4–7) (2002) 539–556.
[11] F.P. Incropera, D.P. DeWitt, T.L. Bergman, A.S. Lavine, Fundamentals of Heat and Mass Transfer, sixth ed., John Wiley & Sons, ISBN: 978-0-471-45728-2, 2007, pp. 260–261.
[12] B. Pateyron, Jets & Poudres, Téléchargeable à partir de: http://jets&poudres.free.fr.
[13] A. Bejan, Convection Heat Transfer, second ed., Wiley, ISBN: 0-471-57972-6, 1994.